Unrestricted superlensing in a triangular two-dimensional photonic crystal

X. Wang, Z. F. Ren and K. Kempa

Department of Physics
Boston College, Chestnut Hill, MA 02467
wangxb@bc.edu

Abstract: We demonstrate unrestricted superlensing in a *triangular* two-dimensional photonic crystal. We investigate simple two-point light sources imaged by a slab lenses made of this photonic crystal, and show that the refraction of light follows simple rules of geometric optics with the Snell's-law refraction at each interface, and an effective *isotropic* refractive index $n=-1$ for light propagating inside the crystal. We contrast this behavior with that of a *square* two-dimensional photonic crystal in the first photonic band, where the effective dielectric response is *anisotropic*. This leads to a restricted superlensing, which does not follow the geometric optics.

OCIS codes: (230.1480) Bragg reflectors; (110.2960) Image analysis

References and links

1. J. B. Pendry, "Negative Refraction Makes a Perfect Lens," Phys. Rev. Lett. **85**, 3966 (2000).
2. J. B. Pendry and S. A. Ramakrishna, "Near-field lenses in two dimensions," J. Phys.: Condens. Matter **14**, 8463 (2002).
3. J.B. Pendry, A.J. Holden, D.J. Robbins, and W.J. Stewart, "Magnetism from conductors and enhanced nonlinear phenomena," IEEE Trans. Microwave Theory Technol. **47**, 2075 (1999).
4. J.B. Pendry, A.J. Holden, W.J. Stewart, and I. Youngs, "Extremely Low Frequency Plasmons in Metallic Mesostructures," Phys. Rev. Lett. **76**, 4773 (1996).
5. D.R. Smith, W.J. Padilla, D.C. Vier, S.C. Nemat-Nasser, and S. Schultz, "Composite Medium with Simultaneously Negative Permeability and Permittivity," Phys. Rev. Lett. **84**, 4184 (2000).
6. R.A. Shelby, D.R. Smith, and S. Schultz, "Experimental Verification of a Negative Index of Refraction," Science **292**, 77 (2001).
7. G. Shvets, "Photonic approach to making a material with a negative index of refraction," Phys. Rev. B **67**, 035109 (2003).
8. A. Grbic and G. V. Eleftheriades, "Experimental verification of backward-wave radiation from a negative refractive index metamaterial," J. Appl. Phys. **92**, 5930 (2002).
9. M. Notomi, "Theory of light propagation in strongly modulated photonic crystals: Refractionlike behavior in the vicinity of the photonic band gap," Phys. Rev. B **62**, 10 696 (2000).
10. S. Foteinopoulou, E. N. Economou, and C. M. Soukoulis, "Refraction in Media with a Negative Refractive Index," Phys. Rev. Lett. **90**, 107402 (2003).
11. S. Foteinopoulou and C. M. Soukoulis, "Negative refraction and left-handed behavior in two-dimensional photonic crystals," Phys. Rev. B **67**, 235107 (2003).
12. C. Luo, S. G. Johnson, J. D. Joannopoulos, and J. B. Pendry, "All-angle negative refraction without negative effective index," Phys. Rev. B **65**, 201104 (2002).
13. P. V. Parimi, W. T. Lu, P. Vodo and S. Sridhar, "Photonic crystals: Imaging by flat lens using negative refraction," Nature (London) **426**, 404 (2003).
14. C. Luo, S. G. Johnson, J. D. Joannopoulos and J. B. Pendry, "Subwavelength imaging in photonic crystals," Phys. Rev. B **68**, 045115 (2003).
15. E. Cubukcu, K. Aydin, E. Ozbay, S. Foteinopoulou, and C. M. Soukoulis, "Electromagnetic waves: Negative refraction by photonic crystals," Nature (London) **423**, 604 (2003).
16. E. Cubukcu, K. Aydin, E. Ozbay, S. Foteinopoulou, and C. M. Soukoulis, "Subwavelength Resolution in a Two-Dimensional Photonic-Crystal-Based Superlens," Phys. Rev. Lett. **91**, 207401 (2003).
17. Zhi-Yuan Li and Lan-Lan Lin, "Evaluation of lensing in photonic crystal slabs exhibiting negative refraction," Phys. Rev. B **68**, 245110 (2003).
18. J. D. Joannopoulos, R. D. Meade, and J. N. Winn, Photonic Crystals: Molding the Flow of Light (Princeton University Press, Princeton, 1995).
19. K. S. Yee, "Numerical solution of initial boundary value problems involving Maxwell's equations in isotropic media," IEEE Trans. Antennas Propag. **14**, 302 (1966).

#4260 - $15.00 US Received 26 April 2004; revised 16 June 2004; accepted 17 June 2004

20. A.Taflove, Computational Electrodynamics—the Finite-Difference Time-Domain Method (Artech House, Norwood, MA, 1995).
21. J. Berenger, "A Perfectly Matched Layer for the Absorption of Electromagnetic Waves," J. Comput. Phys. **114**, 185 (1994).

Materials with isotropic refractive index $n=-1$ have exotic optical properties. Such materials restore not only *phases* of the transmitted propagating waves, but also *amplitudes* of the evanescent waves, that are responsible for the subwavelength details of source geometry, and were proposed to make a superlens capable of subwavelength imaging [1-2]. Since such materials do not exist naturally, proposals have been put forth in recent years to artificially synthesize them. In one scheme [3-6], an effective medium made of metallic rods, and the so-called split-ring resonators, has been shown to act as such a metamedium in the microwave frequency range. Other similar schemes have also been proposed [7-8].

In another approach, it has been shown that a two-dimensional photonic crystal (2D-PC) can act as a metamedium [9-11], however the superlensisng has not been demonstrated. Recently, it was shown that the propagation of light in a square 2D-PC in the first photonic band leads to an all angle negative refraction (AANR), which leads to superlensing, but where an isotropic negative refractive index cannot be defined [12]. The negative refraction and the slab focusing in the second photonic band have recently been demonstrated experimentally in square 2D-PC, again in the microwave frequency range [13]. However, in the theoretical and experimental imaging studies [12-16], the distance between the point source and the edge of the PC slab was less than the lattice constant of the PC. Recently, it was shown that imaging in a square 2D-PC, in the AANR mode, does not follow rules of geometric optics, and that a channeling, rather than isotropic wave propagation occurs inside the PC [17]. This shows that the imaging capabilities are restricted in this PC. In this paper we clarify this issue, and identify a 2D-PC capable of efficient, unrestricted superlensing.

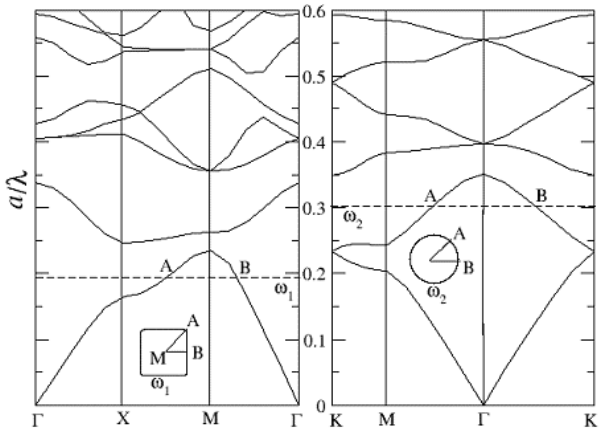

Fig. 1. Calculated photonic band structures for (a) square 2DPC with air-holes of radius $r=0.35a$, in a dielectric matrix with $\varepsilon=12$, and (b) triangular 2DPC with air-holes of radius $r=0.4a$, in a dielectric matrix with $\varepsilon=12.96$. Insets: constant frequency contours for (a) $\omega_1=0.192$ and (b) $\omega_2=0.305$.

The PCs studied in this letter consist of a periodic (in the x-y plane) array of infinitely long, cylindrical (along z-direction) air-holes of radius *r*, embedded in a thick slab of dielectric matrix. Each PC is assumed to have a finite width in the x-direction, but is unrestricted in the y direction. We obtain photonic band structures by numerically solving the Maxwell equations. We employ here the standard plane wave expansion [18]. To obtain maps

#4260 - $15.00 US Received 26 April 2004; revised 16 June 2004; accepted 17 June 2004

of propagating waves, we use the finite-difference time-domain (FDTD) simulations with perfectly matched layer boundary conditions [19-21].

We first study the square PC, which became a structure of choice in the experimental studies of the negative refraction. It was shown, that AANR can occur in this PC [12]. We choose parameters of Ref. [12], i.e., hole radius $r = 0.35a$, where the lattice constant is a, and the dielectric matrix with dielectric constant $\varepsilon = 12$. The calculated band structure (normalized frequency $\omega = a/\lambda$ vs. wave vector k) for the transverse electric (TE) mode (the magnetic field parallel to air holes) is shown in Fig. 1(a). The AANR occurs at the top of the first band (around the M-point), indicated by the horizontal dashed line for $\omega = \omega_1$. The inset in Fig. 1(a) shows the constant frequency contour obtained by crossing the first band with the equal energy surface for $\omega = \omega_1$. The fact that it is not circular, suggest a strong anisotropy of the wave propagation in this PC. As a result, the PC cannot be represented as an effective medium with an isotropic refractive index, and instead a refractive index tensor must be used. In fact, a channeling of the wave propagation in the ΓM and equivalent directions is expected [17], due to larger group velocities of propagating waves in these directions.

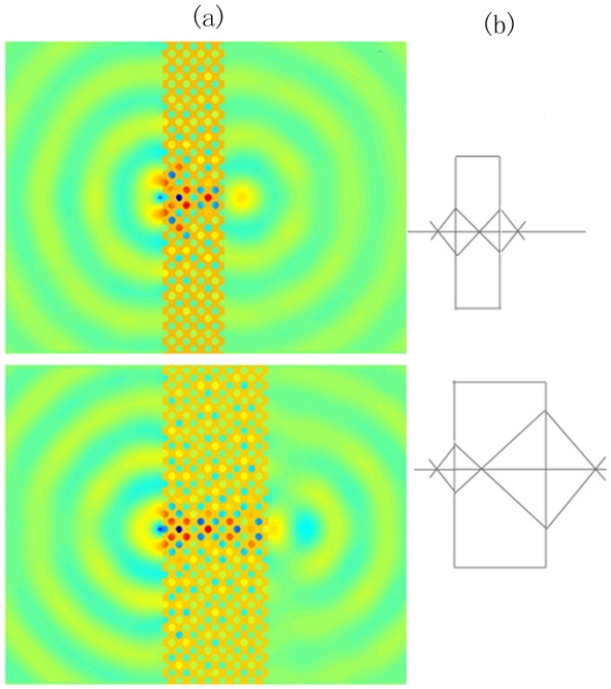

Fig. 2. (a) The propagation map (magnetic field distribution across space) for a slab of the square 2D-PC (the corresponding band structure in Fig.1a), for two thicknesses of the slab, and the point source frequency $\omega_1 = 0.192$. (b) The corresponding sketches of geometric optics analysis, showing that for a thicker slab (lower panel) the image must be further away from the crystal edge.

In order to study this effect in detail, we calculate the wave propagation maps. We turn-on a point source of cylindrical waves with frequency $\omega = \omega_1$ at time t_0, outside and to the left of the slab of the PC, and calculate the field patterns at some later time *t*. Figure 2 shows the calculated magnetic field pattern at the steady state ($t \to \infty$) for two different thicknesses of the slab, and demonstrates that the positions of the image and the source *do not* obey the geometric optics, since in order for this to happen, the distance of the image from the slab

#4260 - $15.00 US Received 26 April 2004; revised 16 June 2004; accepted 17 June 2004

surface would have to be larger for a thicker slab. This is illustrated in Fig. 2 by sketches of geometric optics rays. In fact, a closer inspection of the images shows that instead of the expected focus inside the PC, there is a channel of propagation perpendicular to the slab surface (ΓM direction), in agreement with the argument based on the anisotropy of the equal frequency contour, as discussed above. Increasing the distance of the source from the slab surface, causes the image to disappear inside the slab. By plotting the light intensity across the image, we find that the spatial resolution in this case, as measured by full width at half maximum, is about $t_S = 0.3\lambda$. This all suggests, that the superlensing in this crystal is restricted, and the image formation possible only in the highly non-geometric near-lens mode.

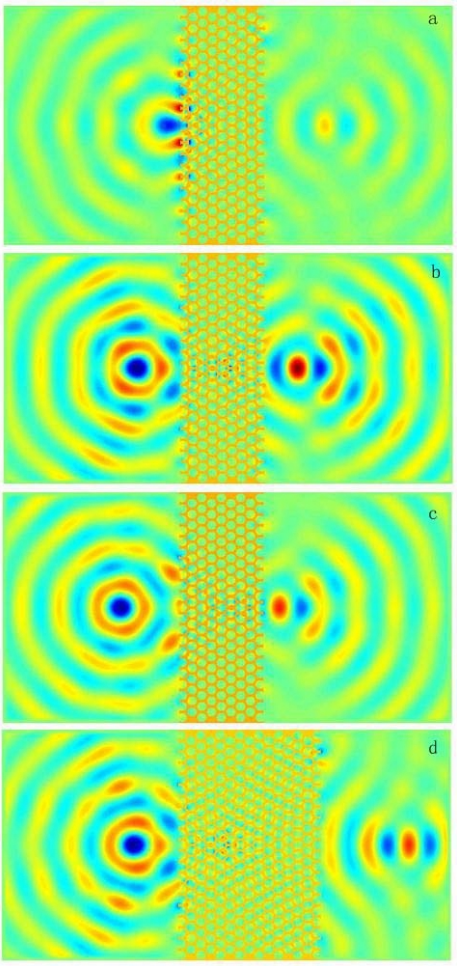

Fig. 3. The propagation map (electric field distribution across space) for a slab of the triangular 2D-PC (the corresponding band structure in Fig.1b), for varying source positions and thickness of the slab. The point source frequency is $\omega_2 = 0.305$. Positions of the images follow the geometric optics analysis, in which the PC is considered a metamedium with $n = -1$, and Snell's-law refraction occurs at each interface.

Let's now consider the *triangular* 2D-PC. Now we choose parameters used in Ref. [9], i.e., $r = 0.4a$ and $\varepsilon = 12.96$. The photonic band structure for the transverse magnetic (TM) modes (the electric field parallel to cylindrical holes) is show in Fig. 1(b). The horizontal dashed line with frequency ω_2 indicates the best frequency for the superlensing.

#4260 - $15.00 US Received 26 April 2004; revised 16 June 2004; accepted 17 June 2004

The corresponding constant frequency contour is now circular. The propagation of the waves is therefore isotropic, and one can define an isotropic effective refractive index. Fig. 3 shows the propagation maps for this case, for various positions of the point source, and thickness of the slab. It can be easily shown, for example by drawing traces of the rays between the sources and the corresponding images, that now the PC acts as a metamedium whit $n=-1$, and therefore the superlensing is *unrestricted*. Again, by plotting light intensity across the image, we find that the spatial resolution in this case is about $t_H = 0.4\lambda$.

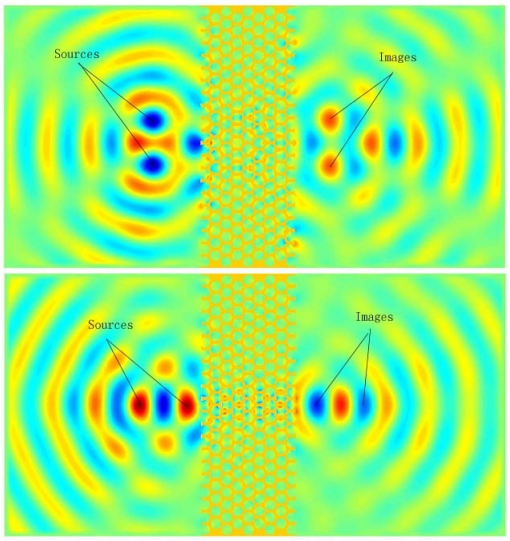

Fig. 4. The propagation map (electric field distribution across space) for a slab of the triangular 2D-PC, for a two point source in a vertical (a), and horizontal (b) positions.

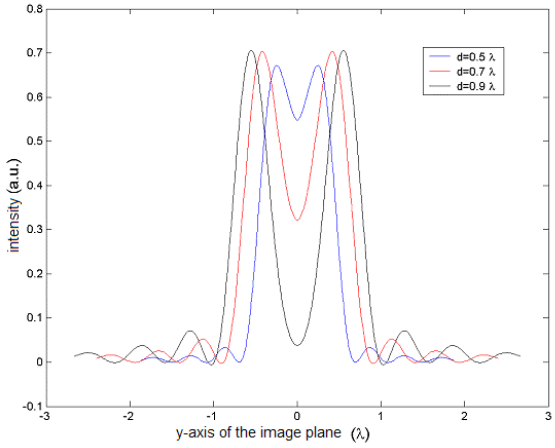

Fig. 5. Light intensity across the image of two vertical point sources for three different distances between sources.

In order to demonstrate the superlens imaging, we show in Fig. 4 wave propagation maps for a two-point source, differently located in front of the slab of the triangular 2D-PC. One obtains clear images of the two points in either horizontal, or vertical configurations. By reducing the distance between the two point sources well below the wavelength, we can test

#4260 - $15.00 US
Received 26 April 2004; revised 16 June 2004; accepted 17 June 2004

the possibility of the subwavelength resolution. Fig. 5 shows the light intensity across the image of two vertical point sources for different distances between the sources.

In conclusion, we show that the imaging is restricted only to the near-lens in the *square* crystal in the AANR mode of operation. We trace this to an *anisotropic* geometry of the constant frequency contour in the relevant section of the photonic band structure. In contrast, we show that in a *triangular* 2D-PC, a highly circular constant frequency contour can be chosen in a relevant band, and as a result an *isotropic* propagation of the refracted waves occurs. Thus this PC can act as an isotropic effective metamedium with an effective refractive index $n=-1$, and therefore capable of unrestricted superlensing. The possibility of improving the spatial resolution of the superlensing will be discussed elsewhere.

Acknowledgments

This work is supported by US Army Research Development and Engineering Command, Natick Soldier Center, under the grant DAAD16-03-C-0052.

#4260 - $15.00 US Received 26 April 2004; revised 16 June 2004; accepted 17 June 2004